Supplement of Earth Syst. Dynam., 16, 169–187, 2025
https://doi.org/10.5194/esd-16-169-2025-supplement

Earth System Dynamics
Open Access
EGU

Supplement of

Future changes in compound explosive cyclones and atmospheric rivers in the North Atlantic

Ferran Lopez-Marti et al.

Correspondence to: Ferran Lopez-Marti (ferran.lopez-marti@geo.uu.se)

S1. JUSTIFICATION FOR THE CHOICE OF 1500 km RADIUS in identifying atmospheric rivers around a cyclone

We have analysed the distribution of the closest points of atmospheric rivers (AR) around the cyclone centre (Fig. S1) and found that most of them fall within the east-southeast quadrant of the 1500 km circle. This is expected, as most ARs that are dynamically associated with a cyclone are located to the southeast of the cyclone centre, linked to the WCB and feeder airstream. This pattern is further illustrated in Figure A2, where the histogram shows that most ARs are in the southeast quadrant. If we expand this radius to 2500 km, there is a shift in AR occurrences toward the southwest and northwest quadrants of the cyclone (Fig. S2), making it less likely that these ARs are dynamically linked to the cyclone. Therefore, we conclude that 1500 km represents a good compromise between maximizing the number of possible cases (statistics) and selecting those that are dynamically linked (dynamics).

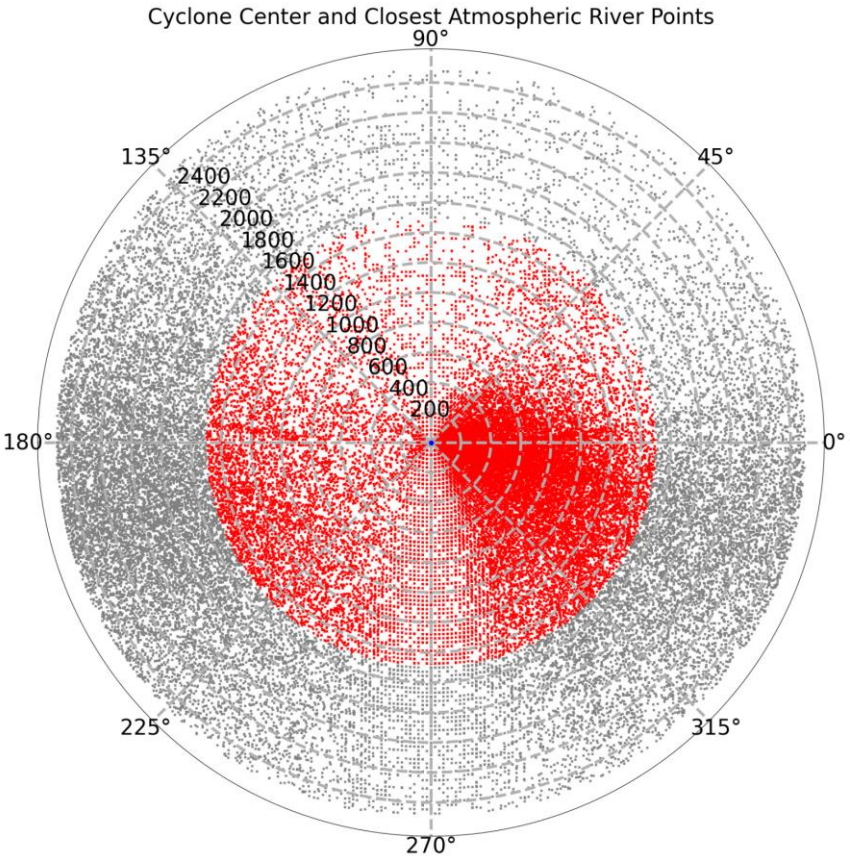

Figure S1. Closest atmospheric river (AR) points found around cyclones, both detected using ERA5 data. Points in red indicate those found within a 1500 km circle from the cyclone center, and in gray those found up to 2500 km away.

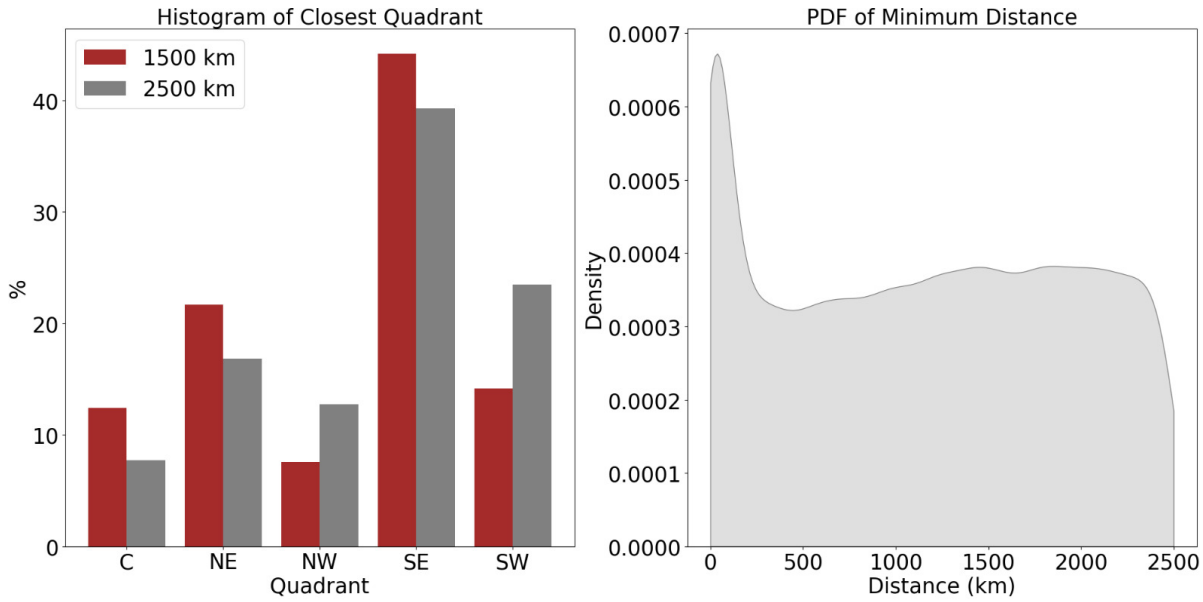

Figure S2. Percentage of occurrence (left) of the cyclone quadrant in which the closest atmospheric river (AR) was found within a 1500 km circle (brown) and a 2500 km circle (gray), for ERA5 data. The right figure shows the probability distribution function (PDF) of the distance, in kilometers, between the cyclone center and the closest point of the AR.

S2. RESOLUTION SENSITIVITY TEST OF ERA5: Impact on the present concurrences of AR with ECs and non-ECs

We performed a sensitivity test where the SLP and IVT fields for ERA5 are interpolated to a 1º, 1.5º and 2º regular lon-lat grid (similar range to the CMIP6 models resolutions). Then the same methodology described in the manuscript is applied to the regridded ERA5. We analysed the sensitivity of the resolution in ERA5 to the concurrence of ARs with ECs and non-ECs as it is done in Fig. 4 a,b (Figures S3 and S4). The rate of coincidence decreases as we reduce the resolution of ERA5 for both EC and non-ECs in the same way. The spread of the regridded ERA5 (1º,1.5º and 2º) is slightly smaller than the spread of the CMIP6 models, but the CMIP6 models do not show lower rate of coincidence for the coarser model resolution. For example, EC-Earth, the model with the highest resolution, shows the lowest concurrence rate of CMIP6 models, or MPI-LH with the lowest resolution has higher concurrences than average. With this sensitivity test we can say that the CMIP6 model spread is not driven by the model resolution since they show different signals. The model spread is driven by the inherent nature of each model (including its resolution), as well as internal variability, and we study it by accounting for the resolution as a characteristic of each model.

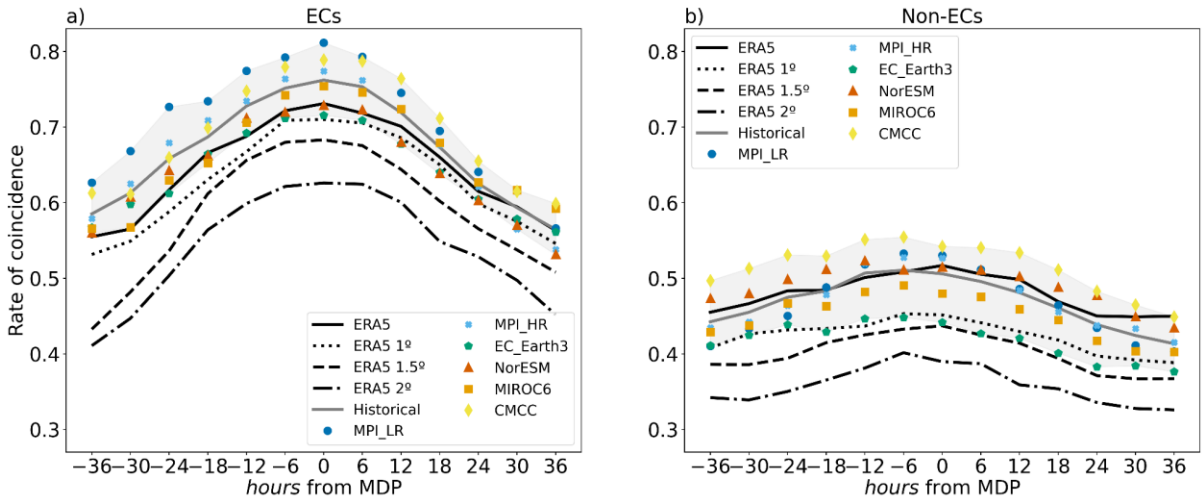

Figure S3. Same as Figure 4a,b of the manuscript but with additional curves for ERA5 interpolated to different resolutions (1º,1.5º and 2º).

We also performed a resolution sensitivity test to the IVT-max results by reproducing Fig. 6 a,b with the regridded ERA5 (Figure S4). The IVT-max values decrease when lowering the resolution in ERA5 for both ECs and non-ECs, the CMIP6 models more or less align with this since higher resolution models show higher IVT-max than the CMPI6 mean and the models with lower resolution show lower IVT-max than the CMPI6 mean. Despite of that, the IVT-max CMIP6 model spread is at least 3 times larger than the regridded ERA5 (1º,1.5º and 2º). Again the model spread is driven by the inherent nature of each model (including its resolution) rather than only the resolution of the model.

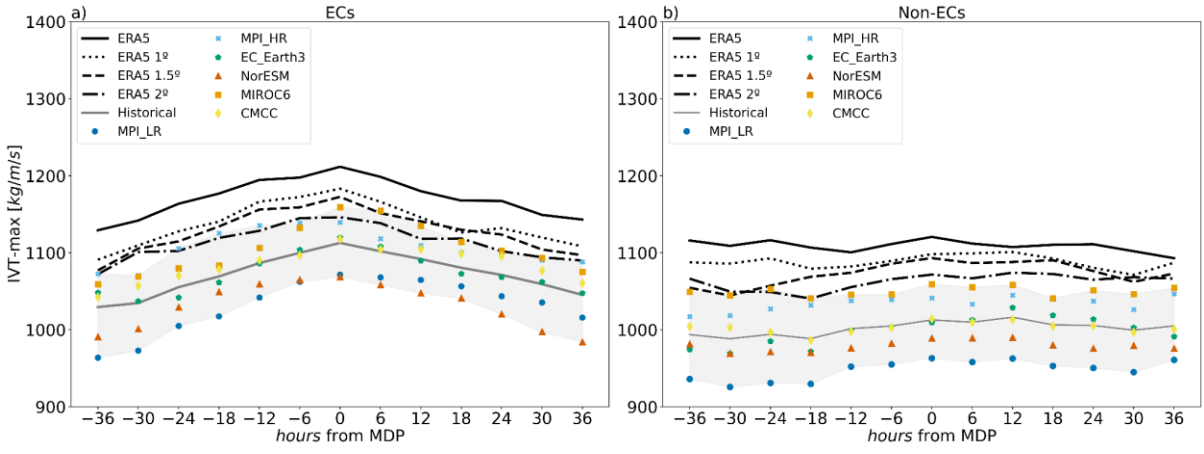

Figure S4. Same as Figure 6a,b of the manuscript but only for historical with additional curves for ERA5 interpolated to different resolutions (1º,1.5º and 2º).

We show in Table S1 the number of AR tracks and EC and non-EC tracks for the regridded ERA5 following the same methodology as in Table A2 and A3. The number of ARs tracks only shows a 5% difference when regridding ERA5 to 2º, suggesting that the "one grid" threshold for the AR tracking has almost no effect on the results. The total number of EC and non-EC tracks show a larger decrease for ERA5 2º but not as much as for ERA5 1º and 1.5º, similar to what we observe between MPI HR and MPI LR. For the other models, the differences in number of cyclone tracks is not proportional to the resolution.

#Tracks	ERA5	ERA5 1º	ERA5 1.5º	ERA5 2º	MPI-HR	MPI-LR	EC-Earth3	NorESM	MIROC6	CMCC-ESM2
AR	1224	1225	1214	1165	1219	1286	1187	1235	1152	1186
non-EC	3200	3391	3240	3092	3046	2387	2927	3594	3424	3530
EC	1372	1307	1262	1158	1168	870	1283	1193	879	1076

Table S1. Number of AR tracks and EC and non-EC tracks following the same methodology as in Table A2 and A3 but for the regridded ERA5.

We acknowledge that differences in model resolution introduce uncertainty, but we consider this an inherent uncertainty of the models themselves. Moreover, when analysing differences between periods, we compare the multi-model means, which is equivalent to comparing each model to itself and then averaging the differences. We never perform a direct comparison across different models. Our main goal here is to assess changes between historical and future scenarios and not model evaluation with ERA5.